ADVANCES IN ATMOSPHERIC SCIENCES, VOL. 32, JULY 2015, 898–908

Low-Level Temperature Inversions and Their Effect on Aerosol Condensation Nuclei Concentrations under Different Large-Scale Synoptic Circulations

LI Jun[1,2], CHEN Hongbin*[1,2], Zhanqing LI[3,4], WANG Pucai[1], Maureen CRIBB[3], and FAN Xuehua[1,2]

[1]*Key Laboratory of Middle Atmosphere and Global Environment Observation, Institute of Atmospheric Physics, Chinese Academy of Sciences, Beijing* 100029

[2]*Collaborative Innovation Center on Forecast and Evaluation of Meteorological Disasters, Nanjing University of Information Science & Technology, Nanjing* 210044

[3]*The Earth System Science Interdisciplinary Center, University of Maryland, College Park, MD* 20740, *USA*

[4]*College of Global Change and Earth System Science, Beijing Normal University, Beijing* 100875

(Received 5 July 2014; revised 23 October 2014; accepted 15 November 2014)

ABSTRACT

Knowledge of the statistical characteristics of inversions and their effects on aerosols under different large-scale synoptic circulations is important for studying and modeling the diffusion of pollutants in the boundary layer. Based on results generated using the self-organizing map (SOM) weather classification method, this study compares the statistical characteristics of surface-based inversions (SBIs) and elevated inversions (EIs), and quantitatively evaluates the effect of SBIs on aerosol condensation nuclei (CN) concentrations and the relationship between temperature gradients and aerosols for six prevailing synoptic patterns over the the Southern Great Plains (SGP) site during 2001–10. Large-scale synoptic patterns strongly influence the statistical characteristics of inversions and the accumulation of aerosols in the low-level atmosphere. The activity, frequency, intensity, and vertical distribution of inversions are significantly different among these synoptic patterns. The vertical distribution of inversions varies diurnally and is significantly different among the different synoptic patterns. Anticyclonic patterns affect the accumulation of aerosols near the ground more strongly than cyclonic patterns. Mean aerosol CN concentrations increase during SBIs compared to no inversion cases by 16.1%, 22.6%, 24.5%, 58.7%, 29.8% and 23.7% for the six synoptic patterns. This study confirms that there is a positive correlation between temperature gradients and aerosol CN concentrations near the ground at night under similar large-scale synoptic patterns. The relationship is different for different synoptic patterns and can be described by linear functions. These findings suggest that large-scale synoptic patterns change the static stability of the atmosphere and inversions in the lower atmosphere, thereby influencing the diffusion of aerosols near the ground.

Key words: temperature inversion, aerosol, condensation nuclei, large-scale synoptic pattern, statistical characteristics

Citation: Li, J., H. B. Chen, Z. Q. Li, C. P. Wang, M. Cribb, and X. H. Fan: Low-level temperature inversions and their effect on aerosol condensation nuclei concentrations under different large-scale synoptic circulations. *Adv. Atmos. Sci.*, **32**(7), 898–908, doi: 10.1007/s00376-014-4150-z.

1. Introduction

Low-level atmospheric temperature inversions, where atmospheric temperature increases with altitude, occur frequently at middle and high latitudes. They influence the depth of vertical mixing, the surface radiation balance, the diffusion of pollutants, and cloud formation in the boundary layer (Fedorovich et al., 1996; Wendisch et al., 1996; Dong et al., 2005; Janhall et al., 2006; Wallace et al., 2010). An inversion in the lower atmosphere creates stable atmospheric conditions, which restricts the diffusion of industrial and human-produced smoke, and harmful gases and aerosols. These pollutants accumulate near the ground, and usually lead to air pollution episodes. Over the past century, several air pollution episodes of major significance have occurred around the world and have led to thousands of deaths. Temperature inversions were mainly responsible for these events (Watanabe, 1998).

Investigation of the effects of low-level temperature inversions on pollutants not only helps us understand the impact of inversions on environmental changes, but also provides a reliable basis for effectively predicting pollution episodes and controlling pollutant emissions. Pollutant gases near the ground, such as CO, NO, NO_2, SO_2 and O_3, significantly increase if a temperature inversion, especially a morning time surface-based temperature inversion (SBI), is present (Holzworth, 1972; Janhall et al., 2006). Aerosols, an important

* Corresponding author: CHEN Hongbin
Email: chb@mail.iap.ac.cn

kind of air pollutant, affect human health, and fine particulate matter ($PM_{2.5}$) mass loadings have been statistically correlated with morbidity and mortality (Pope et al., 1993). The increase in aerosol particle concentrations near the ground is also highly correlated with the presence of temperature inversions (Malek et al., 2006). Wallace et al. (2010) studied the effect of temperature inversions on groud-level NO_2 and aerosols, and reported increases of 49% and 54% in NO_2 and $PM_{2.5}$, respectively, during nighttime inversion episodes. However, which temperature inversion parameters affect the accumulation of aerosols, and the relationship between these parameters and aerosols is still uncertain. Milionis and Davies (1992) found that the intensity of inversions is directly proportional to their ability to inhibit the vertical movement of pollutants. This information is important for modeling the diffusion and transport of air pollutants. Most models of air pollutant diffusion already incorporate characteristics of the capping inversion at the top of the atmospheric boundary layer (ABL) (Milionis and Davies, 2008). However, little attention has been paid to the quantitative assessment of the relationship between inversion parameters and aerosol concentrations.

Serious pollution episodes do not generally result from sudden increases in the emission of pollutants, but rather from certain meteorological conditions that diminish the ability of the atmosphere to disperse pollutants (Cheng et al., 2007). There is a causal relationship between prevailing weather conditions and the statistics describing atmospheric temperature inversions (Milionis and Davies, 2008). Local surface conditions can counteract atmospheric dynamics in regulating inversion activity and air quality. Bailey et al. (2011) analyzed temperature inversion characteristics in the U.S. Southwest and relationships to 500 hPa large-scale atmospheric circulation, and found that dynamical changes with climate did not uniformly influence inversions and urban air quality conditions in that region. Pearce et al. (2011) identified 20 large-scale synoptic patterns over Australia by applying the self-organizing map (SOM) method to daily mean sea level pressure reanalysis data. They found links between synoptic-scale sea level circulation and observed changes in air pollutant concentrations, and that individual synoptic categories had different effects on air pollutants. These studies indicate that changes in large-scale weather patterns can affect low-level temperature inversion statistics and air quality, and that the presence of temperature inversions also prevents pollutants from dispersing. Yet it remains unclear whether the effect of temperature inversion on pollutants is significantly different for different synoptic patterns. The SGP (Southern Great Plains) Central Facility (CF) is located near Lamont in north central Oklahoma and is home to a suite of specialized *in situ* and remote sensing instruments gathering atmospheric data of unprecedented quality, consistency, and completeness. All aerosol and radiosonde data used in this work are from this site. The SGP CF is surrounded by farmland and is distant from large urban areas. However, there are several small cities, one power plant, one oil refinery, and an interstate highway within 50 km of the site. So, atmospheric aerosols over the site can be considered representative of a mixed regional aerosol type. The daily aerosol condensation nuclei (CN) concentrations cycle is strong at the SGP CF. The average aerosol CN concentration near the ground is low and constant during the night, quickly increases during the two hours after sunrise, and reaches its peak in the midafternoon. Possible explanations for the high daytime aerosol CN concentration levels include sulfate formation from SO_2 emissions from local power plants or oil refineries, the photochemically-driven production of organic or N-containing particles, regional-scale agricultural burning or transportation activities, and/or diurnal convective mixing and stability cycles (Sheridan et al., 2001).

The purpose of this work is to quantify inversion activity and its effect on aerosols, and to deduce the relationship between inversion parameters and aerosol CN concentrations for a set of prevailing synoptic patterns over the continental United States. Section 2 briefly describes the data and the method used in this study. The main results are presented in section 3. Conclusions are given in section 4.

2. Data and methods

2.1. *Data*

Ten years (2001–10) of continuous and high-quality routine radiosonde data measured at the SGP CF are used in this study. These measurements are carried out under the aegis of the U.S. Department of Energy's Atmospheric Radiation Measurement Program (www.arm.gov). A Vaisala sounding unit is used to detect vertical profiles of pressure, temperature, relative humidity, and wind speed and direction, four times a day at 0530, 1130, 2030 and 2330 UTC. The profiling vertical resolution is $\sim$10 m (Holdridge et al., 2011). For the purpose of calculating nighttime and daytime temperature inversion parameters, profiles generated from the 2330 UTC sounding represent daytime profiles and 0530/1130 UTC soundings represent nighttime profiles.

Simultaneous ground measurements of aerosol CN and total number concentrations for particles with diameters ranging from 10 nm to 3μm made at a one-minute time resolution are also used (Jefferson, 2011).

For characterizing large-scale synoptic patterns, the daily National Centers for Environmental Protection (NCEP) mean sea level pressure (MSLP) records from the North American Regional Reanalysis (NARR) are used. The MSLP field is a commonly used proxy for atmospheric circulation because it relates well to the spatial pattern of large-scale synoptic processes (Huth et al., 2008). Corresponding daily 500 hPa geopotential heights are also used in the comprehensive analysis presented in this study. The resolution of NCEP NARR products is 32 km $\times$ 32 km and the domain extends from 30°N to 50°N, and from 75°W to 120°W (http://www.esrl.noaa.gov).

2.2. *Algorithm for detecting inversions and the SOM method for weather classification*

This study focuses on low-level inversions with bases below 2000 m. SBIs are inversions with bases below 100 m and elevated inversions (EIs) are inversions with bases above 100 m. The first-derivative algorithm is used here for detecting inversions (Kahl, 1990; Serreze et al., 1992). The derivative of each temperature profile is first calculated. Then, the profile of these derivatives is scanned upward from the surface to the 2000 m level. An inversion layer is identified when the derivative is positive and remains positive over an altitude range of at least 100 m. Very thin negative derivative layers are occasionally encountered. If these layers are less than 100 m, then the thin layers are considered as embedded within the overall inversion layer.

The SOM is an artificial neural network algorithm used for clustering, visualization, and abstraction (Kohonen, 1998). It offers an alternative approach to synoptic climatology by providing a mechanism for visualizing the complex distribution of synoptic states while treating the data as a continuum (Hewitson and Crane, 2002). This technique has been increasingly used to successfully study relationships between local meteorological conditions and the large-scale climatology. The SOM algorithm identifies groups in such a way that minimizes the within-group differences while maximizing the between-group differences. An advantage of this method is that nodes are distributed in a nonlinear fashion. As a result, a larger number of climatological groupings are created near areas of high-density data, allowing one to represent the variability in the original time series of geopotential height records more robustly (Bailey et al., 2011). The use of a small dimension will result in a map that provides a broad generalization of the input data, while a large dimension will result in a map with types that may be quite similar to adjacent types (Cassano et al., 2006). The output dimension selected in this study is based on previous work done on North American weather classification (Hewitson and Crane, 2002; Bailey et al., 2011). Ten years of daily MSLP maps were organized into a 5×5 output dimension through application of the SOM algorithm. The atmospheric state is partitioned into 25 categories associated with large-scale synoptic patterns to provide insight into the influence of large-scale synoptic processes on temperature inversions and aerosols.

The SOM of the MSLP provides a clear visualization of the atmospheric continuum affecting the SGP CF by presenting 25 archetypes of the synoptic state that characterize large-scale atmospheric circulation over the region. The most frequent and representative synoptic patterns are the cyclonic center (CC, also denoted as 00, 7.6%), the weak pressure (WP, also denoted as 02, 6.3%), the cyclonic bottom (CB, also denoted as 04, 4.7%), the cold front (CF, also denoted as 32, 4.7%), the anticyclone edge (AE, also denoted as 34, 5.5%), and the anticyclone center (AC, also denoted as 43, 6.3%). These prevailing synoptic patterns form the basis of the following analysis in this work. Figure 1 shows annual MLSP patterns and their corresponding 500 hPa geopotential height patterns for the six synoptic patterns averaged over 2001 to 2010. In the CC scenario, the SGP CF is located within the area of lowest atmospheric surface pressure (Fig. 1a). A southwesterly flow at the 500 hPa level is seen and is associated with strong convergence and ascending motion in the lowest part of the atmosphere. Weather conditions are mainly overcast with frequent rainfall. In the WP scenario, the SGP CF is within an area of weak depression at the surface and under a 500 hPa ridge (Fig. 1b). Cloudy skies dominate. The SGP CF is located along the edge of a strong depression and near a strong anticyclone in the CB scenario (Fig. 1c). Conditions at the 500 hPa level are similar to those seen in the CC scenario and cloudy skies prevail. Figure 1d shows the CF scenario where the SGP CF is located in the transition zone between warm and cold air masses. Weather conditions are generally rainy and windy with clearing after passage of the front. In the AE scenario, the SGP CF is situated at the rear of a strong anticyclone and the dominant airflow at the 500 hPa level is from the west (Fig. 1e). The sky is clear or contains scattered clouds. The SGP CF is located in the center of anticyclone subsidence in the AC scenario (Fig. 1f). There is a northwesterly flow at the 500 hPa level associated with strong divergence in the lower atmosphere. Clear skies dominate.

3. Results

3.1. *Inversion characteristics*

In order to quantitatively express the relationship between inversion activity and prevailing patterns, a temperature inversion activity index (TIAI) is defined as the product of "mean intensity of inversions (the difference in the potential temperature across the inversion) and average number of inversions per profile where at least one inversion is identified and proportion of temperature profiles with at least one inversion is identified", i.e.,

$$\mathrm{TIAI} = \frac{\sum_{i=1}^{K} d\theta_i}{K} \frac{K}{n} \frac{n}{N} = \frac{\sum_{i=1}^{K} d\theta_i}{N} ,$$

where $d\theta$ denotes the difference in the potential temperature across the inversion, K is the corresponding total number of inversions, i represents one of the corresponding inversions, N is the total number of available vertical temperature inversions, and n is the corresponding number of profiles with at least one inversion (Milionis and Davies, 2008).

According to the synoptic atmospheric classification, the frequencies of the SBI, EI and no-inversion (NIN), and the parameters of the temperature inversions, are calculated for each synoptic pattern using the corresponding temperature profiles. For some profiles, two, three, or four inversions are detected; the SBI and EI occurred together, and all SBI and EI values are considered in this study.

A one-way analysis of variance (ANOVA) is performed to examine whether the mean values of inversion parameters are

statistically significantly different among the six prevailing patterns defined above. Fisher's least significant difference (LSD) test (Fisher, 1966) is also applied, and all differences of pairs of class means are compared with LSDs. A significance level of 0.05 is used. In this work, our null hypothesis (H_0) is that there is no difference in the mean inversion parameters or aerosol concentrations among the six prevailing patterns (groups). H_0 is tested using the F-statistic. When H_0 is rejected, one-way ANOVA can only determine that mean inversion parameters or aerosol concentrations among groups are significantly different, but it does not necessarily confirm that every set of two groups is sufficiently different. The LSD test is a type of multiple comparison test that can investigate this difference between groups. For the application of this test, all differences of two groups are compared using the LSD. When the difference between two group means is greater than the LSD, the two groups are significantly different at the α significance level (0.05).

Table 1 shows the frequencies of occurrence of SBIs and no inversions (NOIs) and the TIAI index of SBIs for the six synoptic patterns. SBIs occur more frequently under anticyclonic patterns (AE: 46.0%; AC: 38.3%) and less frequently under cyclonic patterns (CB: 26.6%; CC: 31.6%) and when a cold front is present (CF: 22.8%). For cyclonic patterns and

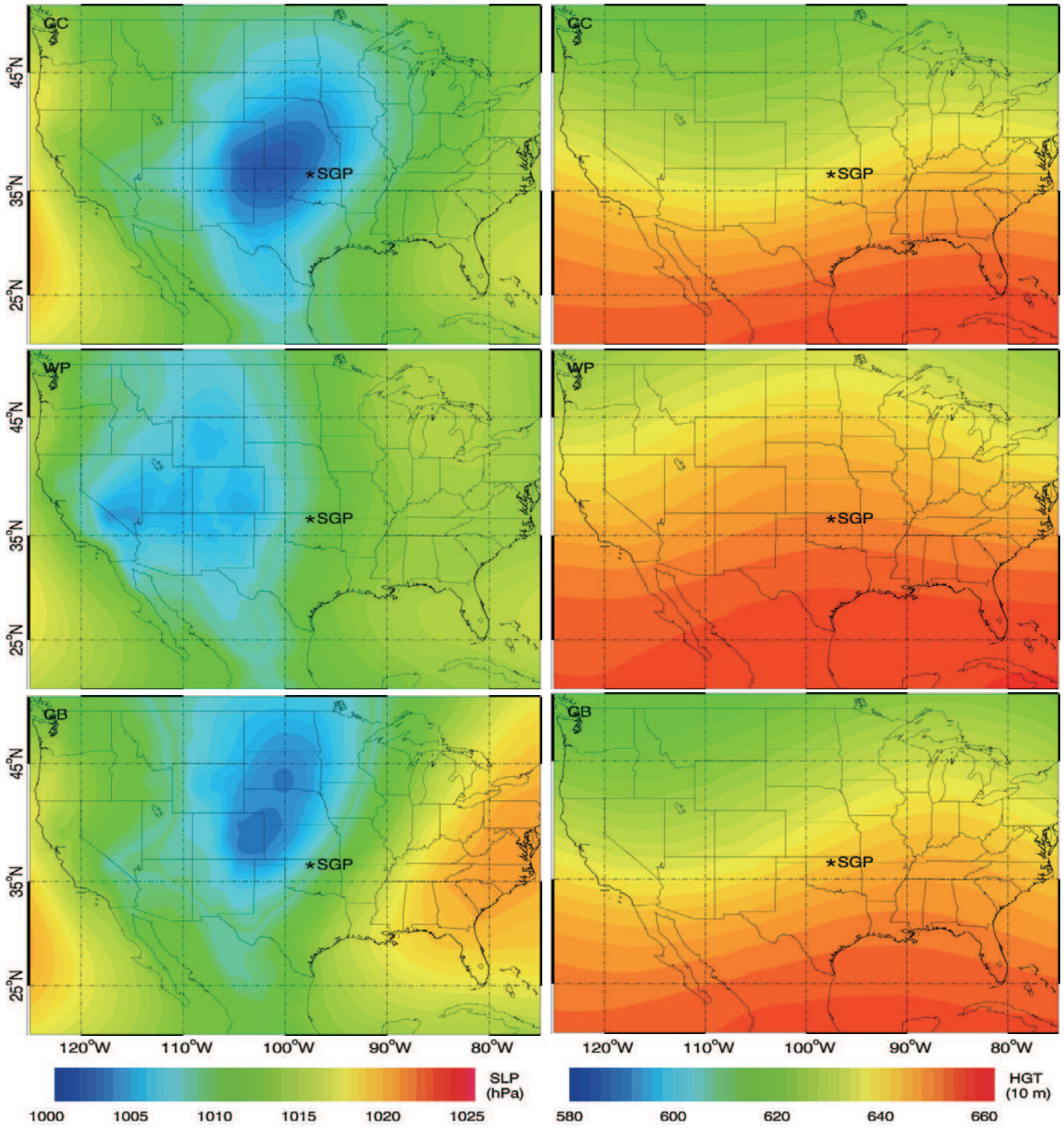

Fig. 1. Annual mean sea level pressure (MSLP) patterns (left column) and their corresponding geopotential height (HGT) patterns (right column) at the 500 hPa pressure level for the six synoptic patterns averaged over 2001 to 2010. CC, WP, CB, CF, AE and AC in the figure stand for patterns of cyclonic center, weak pressure pattern, cyclonic bottom, cold front, anticyclone edge, and anticyclone center, respectively.

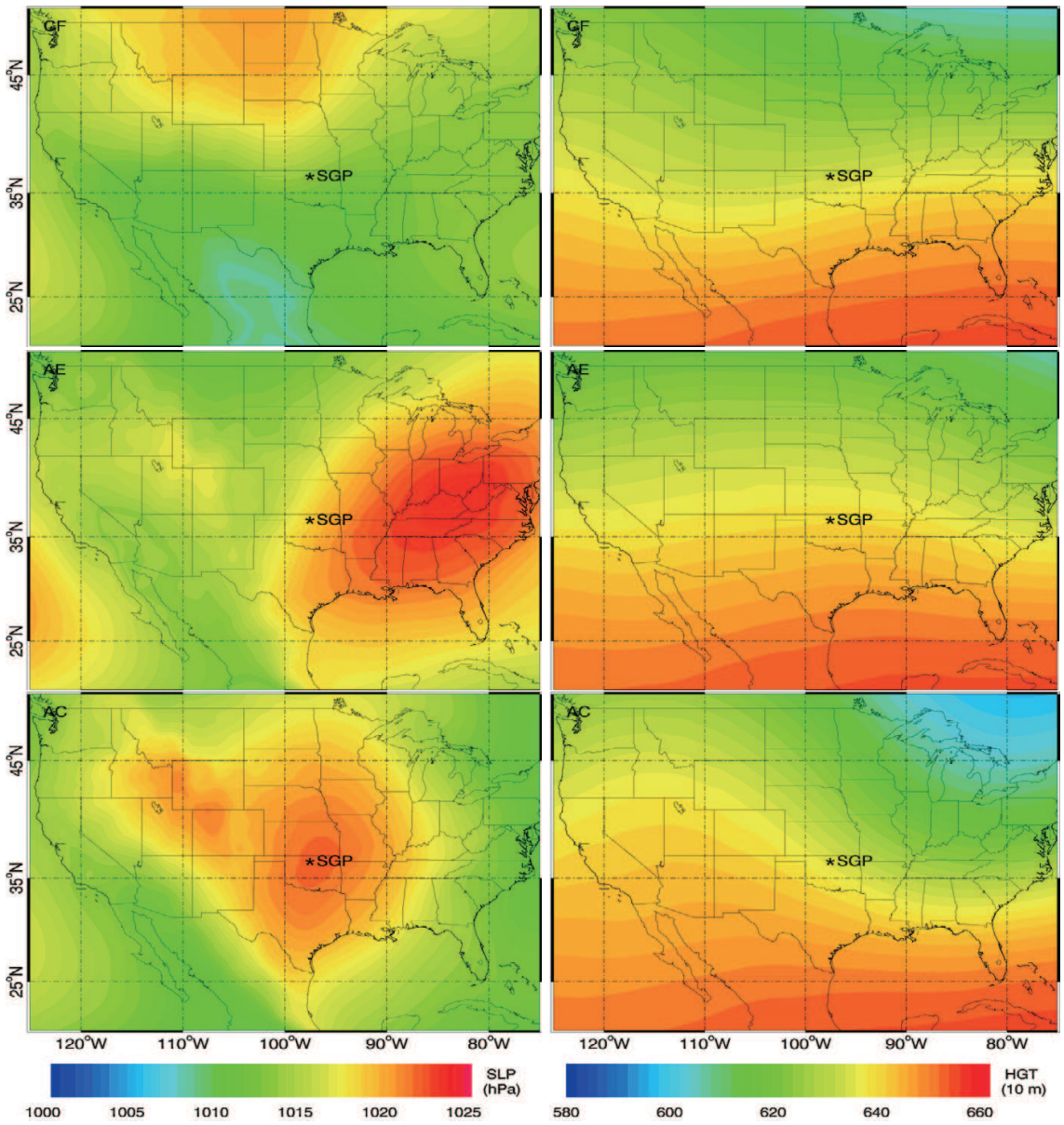

Fig. 1. (Continued.)

weak pressure, the frequency of occurrence of NOIs is high (more than 30%) and that of anticyclonic patterns and cold front is low (less than 20%). Mean TIAI index values of SBIs for the AE and AC patterns are almost twice those for the CB and CF patterns. Table 2 shows mean variances of the SBIs and results from the one-way ANOVA and the LSD test for the six synoptic patterns. Differences in the mean values of temperature difference and temperature gradient across the inversions for the six synoptic patterns are statistically significant at the 95% confidence level (F-values are 17.5 and 32.3, respectively). Differences in mean SBI depths among the different synoptic patterns are small, except for the AC pattern (shaded in gray), which is significantly thinner than the other five patterns. The anticyclonic patterns have the highest values of mean temperature difference across inversions and temperature gradients (shaded in black) and the lowest values are seen for the WP pattern (shaded in gray). In general, anticyclonic patterns favor the formation of SBIs. This pronounced difference may have arisen because anticyclonic patterns are associated with divergence and subsidence near the surface, which increases static stability in the lower atmosphere. The 500 hPa airflow over the SGP CF was from the northwest, bringing in cold and dry air. Under these conditions, clear skies dominated, leading to strong infrared radiation cooling near the ground, which is conducive to the formation and evolution of SBIs. Cyclonic patterns are associated with convergence and ascent near the ground, which decreases static stability in the lower atmosphere. The moist southwesterly air flow at the 500 hPa level leads to cloudy skies with frequent rainfall over the SGP CF. This is generally not conducive to the formation of SBIs. During and after the passage of a cold front at the SGP CF, inclement weather

Table 1. Frequencies of occurrence of SBIs and NOIs and mean TIAI indices of SBIs for the different synoptic patterns.

Synoptic patterns	SBI Frequency (%)	NOI Frequency (%)	SBI TIAI
Cyclonic Center (00)	31.6	35.0	2.49
Weak Pressure (02)	36.2	37.6	2.50
Cyclonic Bottom (04)	26.6	32.2	2.02
Cold Front (32)	22.8	18.6	1.87
Anticyclone Edge (34)	46.0	19.4	4.19
Anticyclone Center (43)	38.3	11.7	3.19

Table 2. Mean depth, temperature difference across the inversion, and temperature gradient for SBIs. Values of SBI characteristics below (above) normal are marked by # (##). The significance level of the F-test is 5%.

	Depth (m)		ΔT(°C)		Temperature gradient [°C (100 m)$^{-1}$]	
Synoptic pattern	Mean	Std	Mean	Std	Mean	Std
CC (00)	266.0	152	5.20	3.6	2.14	1.3
WP (02)	260.9	133	4.31$^{\#}$	2.1	1.99	1.4
CB (04)	275.4	174	4.84	3.4	2.12	2.0
CF (32)	268.6	165	5.47	2.8	2.51	1.6
AE (34)	263.0	169	6.45$^{\#\#}$	3.1	3.07$^{\#\#}$	1.9
AC (43)	216.3$^{\#}$	171	6.17$^{\#\#}$	2.7	3.60$^{\#\#}$	2.1
F-statistics	3.9		17.5		32.3	

Table 3. As in Table 1, but for EIs.

Synoptic pattern	Frequency (%)	Inversions per profile	TIAI
Cyclonic Center (00)	44.2	0.49	2.11
Weak Pressure (02)	35.6	0.37	1.38
Cyclone Bottom (04)	53.5	0.59	2.64
Cold Front (32)	66.9	0.91	5.46
Anticyclone Edge (34)	58.0	0.66	2.63
Anticyclone Center (43)	74.9	1.09	4.61

Table 4. As in Table 2, but for EIs.

	Depth (m)		ΔT(°C)		Temperature gradient [°C (100 m)$^{-1}$]	
Synoptic patterns	Mean	Std	Mean	Std	Mean	Std
CC (00)	211.6$^{\#}$	131	2.71	2.0	1.52	1.2
WP (02)	174.8$^{\#}$	108	2.49$^{\#}$	2.2	1.62	1.0
CB (04)	223.1	124	2.88	1.8	1.45	0.8
CF (32)	251.6	167	3.63$^{\#\#}$	3.1	1.52	0.9
AE (34)	235.0	134	3.22	2.4	1.53	1.1
AC (43)	256.6	155	2.97	2.1	1.30$^{\#}$	0.8
F-statistics	12.9		8.6		5.0	

develops. SBIs rarely occur under these weather conditions. However, before the passage of a cold front, the site is located within a warmer air mass, and winds are calm. The lower atmosphere is statically stable and SBIs can develop. The intensity of SBIs before a cold frontal passage is somewhat weaker than that under the anticyclonic pattern.

Tables 3 and 4 show the same information as Tables 1 and 2, but for EIs. EIs and SBIs have significantly different characteristics, especially with regard to mean temperature differences and temperature gradients across inversions. The frequency of occurrence of profiles with at least one inversion, the average number of inversions per profile, the mean depth, and the mean temperature difference across inversions are highest in magnitude for anticyclonic and CF patterns (shaded in black), and are lowest in magnitude for the AC and WP patterns. Intermediate values are seen for the CB pattern (shaded in gray). TIAI index values for EIs range from 1.38 to 5.46 for the WP and CF patterns, respectively. The difference in temperature gradients of EIs among all patterns is small (F-value = 5.0), and the mean temperature gradient under the AC pattern is significantly lower than that under the other five synoptic conditions. The inversion strength and activity of EIs are comparatively higher for anticyclonic patterns because these patterns are associated with air subsiding in the lower troposphere and gradually spreading over a wide area. Warming by adiabatic compression occurs and inversions are then formed. SBIs are destroyed by turbulence near the surface after sunrise, which leads to EIs separated from the ground. The strength and activity of EIs under the CF pattern is the highest because cold front systems are associated with polar air masses moving into lower latitudes. A polar air mass is colder than the air aloft, so creates stronger EIs. Convergence and upward motion in the lower troposphere associated with cyclonic conditions decreases static stability, which is not conducive to the formation of EIs.

The vertical distribution of inversion characteristics according to the synoptic pattern was examined. High vertical resolution radiosonde profiles used in this work can provide detailed information about the vertical distribution of inversions in the lower atmosphere. Figure 2 shows the vertical distribution of daytime and nighttime frequencies of occurrence of inversions from the surface to 2 km for the six synoptic patterns. The distributions of nighttime inversion frequency for all synoptic patterns have a pronounced maximum from the ground to 100 m (Fig. 2a). The rate of decrease with height is relatively higher above 100 m and inversion frequencies for all synoptic patterns are less than 5% beyond 1300 m. For AC and WP patterns, the frequency of inversions is greater than 70% and the rate of decrease with height is also significantly higher below 500 m when compared to cyclonic and CF patterns. The vertical distributions of daytime inversion frequency for the six synoptic patterns are quite different from the nighttime cases (Fig. 2b). There are almost no SBIs near the ground and inversion frequencies rapidly increase with height, reaching maximum values from 300 to 700 m. Inversion frequencies for the anticyclonic pattern peak between 300 m and 500 m. No clear maximum in inversion frequency below 2 km is seen for the CC and WP patterns. For the CF and CB patterns, inversion frequencies are higher and reach a maximum between 500 m and

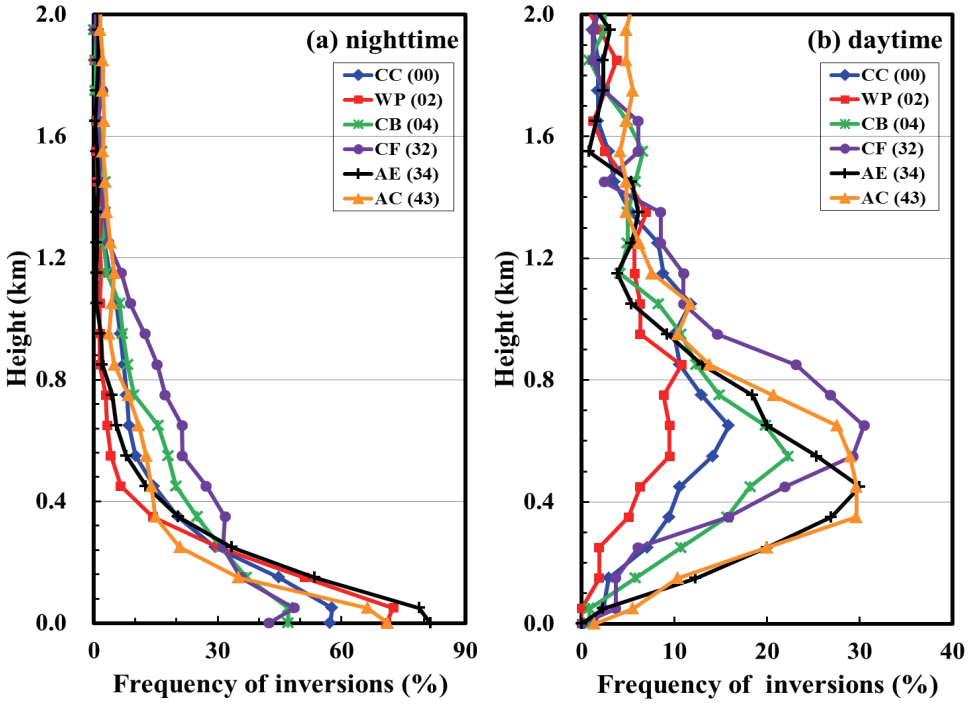

Fig. 2. Vertical distributions of (a) nighttime and (b) daytime frequencies of occurrence of inversions below 2 km for the six synoptic patterns.

700 m. The effect of synoptic patterns on the vertical distribution of inversions is summarized as follows. Anticyclonic and WP patterns are associated with a stable low-level atmosphere and clear skies, which is conducive to the formation of shallow and strong radiation inversions at night. Subsidence in the lower atmosphere is stronger for anticyclonic patterns, which leads to favorable conditions for the formation of EIs at night and during the day. Cyclonic patterns are associated with an unstable lower atmosphere and cloudy skies, which is not conducive to the formation of SBIs and EIs during both daytime and nighttime. CF and CB patterns are associated with cold air invasions, which are favorable conditions for the development of EIs, but not of SBIs.

Overall, large-scale synoptic patterns strongly affect the activity, intensity, and vertical distribution of both SBIs and EIs. There is a significant difference in the vertical distribution of daytime and nighttime inversions. Anticyclonic patterns are associated with maxima in activity and intensity, and cyclonic patterns are associated with minima in activity and intensity for both SBIs and EIs. The CF pattern is conducive to the development of EIs, but not to the formation of SBIs.

3.2. *Effect of inversions on aerosol concentrations*

The physical and chemical processes involved in the formation of aerosol CN are complex, especially during the day. Sources of mixed regional aerosols at the SGP CF may include sulfates from the oil refinery, power plant, and vehicular traffic SO_2 emissions, smoke from local/regional agricultural burning, dust from desert regions, and the photochemically-driven production of organic or N-containing particles. Meteorological parameters such as wind, cloud, relative humidity, and precipitation strongly influence the formation and transportation of aerosols, and are dependent on the large-scale synoptic pattern. Under the same large-scale synoptic atmospheric circulation conditions, especially at night, the effects of the above factors on the formation and transportation of aerosols are similar. Therefore, the following analysis is mainly focused on the accumulation of aerosol CN concentrations and its relationship with nighttime inversions for different large-scale synoptic patterns.

Table 5 shows the results of the one-way ANOVA and the

Table 5. Results from the one-way ANOVA and the LSD test for differences in mean aerosol CN concentrations in the presence of an SBI, an EI, and when there is no inversion (NOI) during nighttime.

	Night aerosol CN concentrations (cm^{-3})		
SGP	Total	Mean	SD
SBI	3079	4900	2121
EI	1000	3698	1928
NOI	538	3849	2023
F		159.1	

LSD Test		DM	LSD	SSD
	SBI & NOI	193	1051	Yes
	SBI & EI	148	1203	Yes
	EI & NOI	206	152	No

*NOI: no inversion; DM: difference in means; SSD: statistically significant difference. LSD test at the 0.05 significance level.

Table 6. Mean aerosol concentrations for all profiles, all nighttime profiles only, nighttime SBIs, nighttime profiles without SBIs, and increasing rates in aerosol concentrations (in %) for the six synoptic patterns. Mean aerosol concentrations below (above) normal are marked by # (##). The significance level of the F-test is 5%.

	Aerosol concentrations (cm^{-3})										
	All		Night		Night SBI		Night EI		Night No-SBI		
Weather patterns	Mean	Std	Mean	Std	Mean	Std	Mean	Std	Mean	Std	Increasing rate (%)
CC (00)	4099	2564	3799	1967	4041#	2042	3272#	1640	3480	1820	16.1
WP (02)	4202	2147	4247	1796	4523#	1808	3987	1802	3688	1644	22.6
CB (04)	4306	2548	4054	1889	4526	2105	3633	1673	3635	1567	24.5
CF (32)	4512	2987	4063	2341	5181	2382	3301	1904	3264	1963	58.7
AE (34)	5252##	2486	5318##	2233	5544	2252	4568##	1961	4271	1823	29.8
AC (43)	5471##	2809	4908##	2048	5217	1968	4313##	1948	4239##	2067	23.7
F	28.1		23.2		14.3		5.2		4.1		

LSD test for differences in the mean aerosol CN concentrations in the presence of an SBI, an EI, and when there is no inversion using 10 years of nighttime radiosonde profiles without considering synoptic patterns. At night, the F-statistic is 159.1, which means that mean aerosol CN number concentrations are statistically correlated with the presence of an SBI at the 95% confidence level. The various LSD tests results show that there are significant differences in mean aerosol CN number concentrations for the SBI/NOI and SBI/EI cases (difference in means, DM $<$ LSD). For the EI/NOI case, however, there is no significant difference (DM $>$ LSD).

Table 6 summarizes the mean aerosol CN concentrations from all profiles, all nighttime profiles only, nighttime profiles containing SBIs only, nighttime profiles containing EIs only, and nighttime profiles without SBIs (including EI and NOI) for the six synoptic patterns. Statistical differences in aerosol CN concentrations among the synoptic patterns were also examined by applying one-way ANOVA and the LSD test. Differences in mean aerosol CN concentrations for the six synoptic patterns are statistically significant at the 95% confidence level, except when there are no SBIs (F-value = 4.1). AC and AE patterns have the highest values of mean aerosol CN concentrations (shaded in black), and cyclonic patterns (CC, CB, and WP) have the lowest values of mean aerosol CN concentrations. This difference is particularly significant for "all profiles" and "nighttime only" profiles (F-values are 28.1 and 23.2, respectively). Mean aerosol CN concentrations for AC and AE patterns are over 5000 cm^{-3}, which is significantly higher than those for the other synoptic patterns. Mean aerosol CN concentrations during the night with SBIs, EIs, and without SBIs are similar, but the overall difference is smaller (F-values are 14.3, 5.2, and 4.1, respectively).

Another important feature of the results presented in Table 6 is the impact of SBIs and EIs on aerosols for the six synoptic patterns. Aerosol CN concentrations in the presence of an SBI, an EI, and when there is no SBI are examined using the above statistical methodology. F-values for all categories are greater than 7.0 and LSD tests also show that there are significant differences in mean aerosol CN number concentrations for the SBI/no-SBI and SBI/EI classes. In order to quantitatively assess this impact, mean aerosol CN concentrations during the night with and without SBIs were compared. Mean aerosol CN concentrations when nighttime SBIs are present are significantly greater than those without SBIs for all synoptic patterns, and the increase in percentage is different. For anticyclonic patterns, mean aerosol CN concentrations are the greatest whether an SBI occurred or not. Mean aerosol CN concentrations when an SBI is present are 23.7% and 29.8% higher than when there is no SBI for AC and AE patterns, respectively. For cyclonic patterns, mean aerosol CN concentrations are lower whether an SBI occurred or not. Percentage increases for CC, WP, and CB patterns are 16.1%, 22.6%, and 24.5%, respectively. The mean aerosol CN concentrations for the CF pattern is 58.7% higher when an SBI is present than when there is no SBI. This is the highest percentage value calculated for all patterns.

The differences in aerosol mean CN concentrations for anticyclonic synoptic patterns can be attributed to the enhancement of static stability in the lower atmosphere under anticyclonic synoptic conditions, which constrains the diffusion of aerosols and favors the accumulation of aerosols near the ground. Cyclonic synoptic patterns associated with convergence and ascending motion near the ground are conducive to the vertical transport and diffusion of aerosols. TIAI index values and temperature gradients of SBIs for cyclonic synoptic patterns are relatively low, so the ability of SBIs to trap aerosols near the ground is weaker. For anticyclonic synoptic patterns, the activity and static stability of SBIs are relatively stronger, so SBIs can more effectively constrain the diffusion of aerosols to near the ground. The activity and static stability of SBIs is strong before the passage of a cold front, and almost all SBIs occurred under these conditions, so aerosol CN concentrations at the SGP CF were particularly high then. After the passage of a cold front, aerosol CN concentrations reduce rapidly, due to scavenging effects of the cold front on aerosols. This explains why mean aerosol CN concentrations when SBIs are present are much higher than when no SBI is present for the CF pattern.

The analysis of the effects of SBIs on aerosol CN concentrations presented above demonstrates that the static stability in the lower atmosphere directly affects the accumulation of

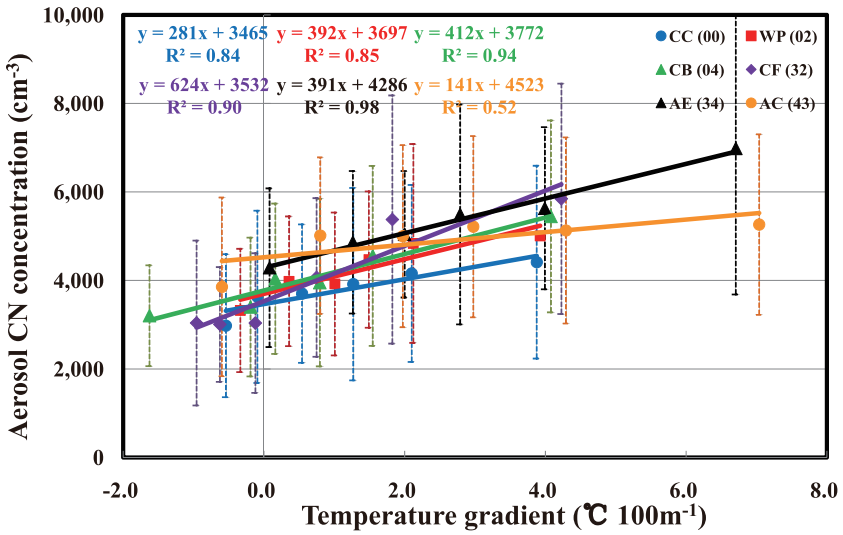

Fig. 3. Aerosol CN concentrations as a function of temperature gradient in the lower atmosphere for the six synoptic patterns. Color-coded linear regression functions are shown.

aerosols near the ground. Li (2012) confirmed that the temperature gradient is the most relevant of inversion parameters with regard to the nighttime surface accumulation of aerosols. A quantitative examination of the relationship between temperature gradient (rate of temperature increase across an SBI or from the surface to 300 m above) and aerosol CN concentrations at night for different synoptic patterns was done. Figure 3 shows that a positive linear relationship exists between temperature gradient and aerosol CN concentrations for all six synoptic patterns. The slopes of the linear equations represent the rate of change of aerosol CN concentrations with temperature gradient and the intercepts represent mean aerosol CN concentrations in a quasi-neutral lower atmosphere. This confirms that the temperature gradient directly affects the diffusion of aerosols near the ground. Mean aerosol CN concentrations in a quasi-neutral lower atmosphere and rates of aerosol change are different for different synoptic patterns. For the CC pattern, both the rate of aerosol change [281 $\mathrm{cm}^{-3}\ ^{\circ}\mathrm{C}^{-1}\ (100\ \mathrm{m})^{-1}$] and mean aerosol concentrations (3465 cm^{-3}) are low, so the effect of this synoptic atmospheric circulation pattern on aerosols is weak. For the WP, CB, and AC patterns, rates of aerosol change are almost the same [$\sim$400 $\mathrm{cm}^{-3}\ ^{\circ}\mathrm{C}^{-1}\ (100\ \mathrm{m})^{-1}$] and significantly higher than seen when a CC pattern is present. Mean aerosol CN concentrations are different, so the ability of SBIs to trap aerosols near the ground is stronger. The rate of aerosol change under CF conditions [624 $\mathrm{cm}^{-3}\ ^{\circ}\mathrm{C}^{-1}\ (100\ \mathrm{m})^{-1}$] is the highest because the passage of a cold front dramatically changes the static stability in the lower atmosphere. Contrary to expectations, the rate of aerosol change for the AC pattern [141 $\mathrm{cm}^{-3}\ ^{\circ}\mathrm{C}^{-1}\ (100\ \mathrm{m})^{-1}$] is the lowest ($R^2 = 0.52$). An explanation may be that this kind of synoptic pattern is associated with strong horizontal divergence and subsidence in the lower troposphere. This synoptic pattern is conducive to the accumulation of aerosols near the ground, so the effect of SBIs on aerosols is independent of temperature gradient.

The influence of synoptic patterns on aerosol CN concentrations is strong. Anticyclonic patterns are associated with higher aerosol concentrations and cyclonic patterns are associated with lower aerosol concentrations. The presence of an SBI results in increased aerosol CN concentrations for all synoptic patterns, but the magnitude of the change in aerosol CN concentrations is different among the different synoptic patterns. The passage of a cold front has a strong scavenging effect on aerosols. There are significant relationships between temperature gradient and aerosol CN concentrations under the same large-scale synoptic pattern, and these relationships are different for different synoptic patterns. This information may be useful for air pollution diffusion modeling.

4. Conclusions

Using the SOM weather classification method, 10 years of atmospheric profiles and aerosol CN concentration data from the SGP CF and the sea level pressure product from the NARR were used to examine the statistical characteristics of inversions and to quantify the impact of inversions on aerosol CN concentrations for different large-scale synoptic patterns. The main findings are:

(1) The highest frequency, activity, and intensity of SBIs are associated with anticyclonic patterns. EIs occur most frequently and are more intense under anticyclonic and CF conditions.

(2) An examination of the vertical distributions of inversion frequency for the six synoptic patterns further confirms that synoptic patterns affect the activity and intensity of inversions. The vertical distribution of inversions varies diurnally. At night, a peak in inversion frequency is seen between the ground and 100 m, and during the day, a peak is seen between 300 m and 700 m.

(3) Mean aerosol CN concentrations are highest for anti-

cyclonic patterns and are lowest for cyclonic patterns. This is partly because anticyclonic conditions increase the static stability in the lower atmosphere and cyclonic conditions are associated with convergence and ascending air motion near the ground. During the night, SBIs are one of the key factors that influence the accumulation of aerosols. The degree of change in aerosol CN concentrations is greater for anticyclonic patterns than for cyclonic patterns, and is the highest for the CF pattern.

(4) The temperature gradient in the lower atmosphere correlates fairly well with aerosol concentrations near the ground for all synoptic patterns, but rates of aerosol concentration change with temperature gradient are significantly different. The rate of aerosol concentration change is $\sim$400 cm^{-3} °C^{-1} (100 m)$^{-1}$ for the WP, CB and AC patterns, and $\sim$280 cm^{-3} °C^{-1} (100 m)$^{-1}$ for the CC pattern. Due to the strong scavenging effect of a cold front, the rate of aerosol concentration change is the highest [$\sim$620 cm^{-3} °C (100 m)$^{-1}$] under this synoptic condition. The lowest rate of aerosol concentration change [140 cm^{-3} °C (100 m)$^{-1}$] is found when an AC atmospheric circulation pattern is in place.

Overall, these results provide strong evidence regarding the behavior of inversions and their effects on aerosols for different large-scale synoptic patterns and provide general insight into the relationship between temperature gradients in the lower atmosphere and aerosols near the ground. Quantitative assessments of inversion statistics, the impact of SBIs on aerosol CN concentrations, and the relationships between temperature gradients and aerosol concentrations are important for modeling and predicting the diffusion of aerosols near the ground under different synoptic conditions. A generalized additive model approach is an effective tool to develop air pollutant models based on historical pollutant concentrations, and meteorological and other relevant data. This approach has been used to model and predict daily air pollutants (Carslaw et al., 2007). Using the results of this study combined with the generalized additive model approach, we plan to develop aerosol diffusion models to more effectively assess relationships between inversions and aerosols, and to more accurately predict aerosol concentrations near the ground under different large-scale synoptic atmospheric circulation conditions.

Acknowledgements. The data used in this work were made available by the Atmospheric Radiation Measurement (ARM) Program sponsored by the U.S. Department of Energy (DOE). This work was supported by the Ministry of Science and Technology of China (Grant Nos. 2010CB950804 and 2013CB955801), the "Strategic Priority Research Program" of the Chinese Academy of Sciences (Grant No. XDA05100300), and the National Natural Science Foundation of China (Grant No. 41305011).

REFERENCES

Bailey, A., T. N. Chase, J. J. Cassano, and D. Noone, 2011: Changing temperature inversion characteristics in the US Southwest and relationships to large-scale atmospheric circulation. *J. Appl. Meteor. Climatol.*, **50**(6), 1307–1323.

Carslaw, D. C., S. D. Beevers, and J. E. Tate, 2007: Modeling and assessing trends in traffic-related emissions using a generalized additive modeling approach. *Atmos. Environ.*, **41**(26), 5289–5299.

Cassano, J. J., P. Uotila, and A. Lynch, 2006: Changes in synoptic weather patterns in the polar regions in the twentieth and twenty-first centuries, Part 1: Arctic. *Inter. J. Climatol.*, **26**(8), 1027–1049.

Cheng, C. S. Q., and Coauthors, 2007: A synoptic climatological approach to assess climatic impact on air quality in south-central Canada. Part I: Historical analysis. *Water Air, and Soil Pollution*, **182**(1–4), 131–148.

Dong, X. Q., P. Minnis, and B. K. Xi, 2005: A climatology of midlatitude continental clouds from the ARM SGP Central Facility: Part I: Low-level cloud microphysical, microphysical, and radiative properties. *J. Climate*, **18**(9), 1391–1410.

Fedorovich, E., P. Kaiser, M. Rau, and E. Plate, 1996: Wind tunnel study of turbulent flow structure in the convective boundary layer capped by a temperature inversion. *J. Atmos. Sci.*, **53**(9), 1273–1289.

Fisher, R. A., 1966: *The Design of Experiments*. 8th ed., Hafner Publishing Company, New York, 248 pp.

Hewitson, B. C., and R. G. Crane, 2002: Self-organizing maps: Applications to synoptic climatology. *Climate Research*, **22**(1), 13–26.

Holdridge, D., J. Prell, M. Ritsche, and R. Coulter, 2011: Balloon-borne sounding system (BBSS) handbook. DOE ARM Tech. Rep. TR-029, 11 pp. [Available online at http://www.arm.gov/publications/tech_reports/handbooks/sonde_handbook.pdf?id=66.]

Holzworth, G. C., 1972: Vertical temperature structure during 1966 Thanksgiving week air-pollution episode in New York City. *Mon. Wea. Rev.*, **100**(6), 445–450.

Huth, R., C. Beck, A. Philipp, M. Demuzere, Z. Ustrnul, M. Cahynov, J. Kysely, and O. E. Tveito, 2008: Classifications of atmospheric circulation patterns recent advances and applications. *Trends and Directions in Climate Research*, L. Gimeno, R. Garcia-Herrera, and R. M. Trigo, Eds., Blackwell Publishing, Oxford, 105–152.

Janhall, S., K. F. G. Olofson, P. U. Andersson, J. B. C. Pettersson, and M. Hallquist, 2006: Evolution of the urban aerosol during winter temperature inversion episodes. *Atmos. Environ.*, **40**(28), 5355–5366.

Jefferson, A., cited 2014: Aerosol observing system handbook. [Available online at http://www.arm.gov/Publications/tech_reports/handbooks/aos_handbook.pdf.]

Kahl, J. D., 1990: Characteristics of the low-level temperature inversion along the Alaskan Arctic coast. *Inter. J. Climatol.*, **10**(5), 537–548.

Kohonen, T., 1998: The self-organizing map. *Neurocomputing*, **21**, 1–6.

Li. J., 2012: Analysis of the interactions between atmospheric temperature inversion and aerosols using ARM data. PhD Thesis, Key Laboratory of Middle Atmosphere and Global Environment Observation, Institute of Atmospheric Physics, Chinese Academy of Sciences, 60–65.

Malek, E., T. Davis, R. S. Martin, and P. J. Silva, 2006: Meteorological and environmental aspects of one of the worst national air pollution episodes (January, 2004) in Logan, Cache Valley, Utah, USA. *Atmospheric Research*, **79**(2), 108–122.

Milionis, A. E., and T. D. Davies, 1992: A 5-Year climatology of

elevated inversions at Hemsby (UK). *Inter. J. Climatol.*, **12**(2), 205–215.

Milionis, A. E., and T. D. Davies, 2008: The effect of the prevailing weather on the statistics of atmospheric temperature inversions. *Inter. J. Climatol.*, **28**(10), 1385–1397.

Pearce, J. L., J. Beringer, N. Nicholls, R. J. Hyndman, P. Uotila, and N. J. Tapper, 2011: Investigating the influence of synoptic-scale meteorology on air quality using self-organizing maps and generalized additive modeling. *Atmos. Environ.*, **45**(1), 128–136.

Pope, C. A., D. W. Dockery, X. Xu, F. E. Speizer, J. D. Spengler, and B. G. Ferris, 1993: Mortality risks of air-pollution-a prospective cohort study. *Am. Rev. Respir. Dis.*, **147**(4), A13–A13.

Serreze, M. C., J. D. Kahl, and R. C. Schnell, 1992: Low-level temperature inversions of the Eurasian Arctic and comparisons with Soviet drifting station data. *J. Climate*, **5**(6), 615–629.

Sheridan, P. J., D. J. Delene, and J. A. Ogren, 2001: Four years of continuous surface aerosol measurements from the Department of Energy's Atmospheric Radiation Measurement Program Southern Great Plains Cloud and Radiation Testbed site. *J. Geophys. Res.*, **106**(D18), 20735–20747.

Wallace, J., D. Corr, and P. Kanaroglou, 2010: Topographic and spatial impacts of temperature inversions on air quality using mobile air pollution surveys. *Science of the Total Environment*, **408**(21), 5086–5096.

Watanabe, O., 1998: Air Pollution Control Technology Manual. [Available online at https://www.env.go.jp/earth/coop/coop/document/01-apctme/contents.html]

Wendisch, M., S. Mertes, A. Ruggaber, and T. Nakajima, 1996: Vertical profiles of aerosol and radiation and the influence of a temperature inversion: Measurements and radiative transfer calculations. *J. Appl. Meteor.*, **35**(10), 1703–1715.